Giant spin-orbit splitting in a HgTe quantum well

Y. S. Gui,[1,2] C. R. Becker,[1,*] N. Dai,[2] J. Liu,[1] Z. J. Qiu,[2] E. G. Novik,[1] M. Schäfer,[1] X. Z. Shu,[2] J. H. Chu,[2] H. Buhmann,[1] and L. W. Molenkamp[1]

[1]*Physikalisches Institut der Universität Würzburg, Am Hubland, 97074 Würzburg, Germany*

[2]*National Laboratory for Infrared Physics, Shanghai Institute of Technical Physics, Chinese Academy of Sciences, Shanghai 200083, China*

(Received 4 May 2004; published 27 September 2004)

We have investigated beating patterns in Shubnikov–de Haas oscillations for $HgTe/Hg_{0.3}Cd_{0.7}Te(001)$ quantum wells with electron densities of $2-3\times10^{12}$ cm^{-2}. Up to 12 beating nodes have been observed at magnetic fields between 0.9 and 6 T. Zero-magnetic-field spin-orbit splitting energies up to 30 meV have been directly determined from the node positions as well as from the intersection of self-consistently calculated Landau levels. These values, which exceed the thermal broadening of Landau levels, k_BT, at room temperature, are in good agreement with Rashba spin-orbit splitting energies calculated by means of an 8×8 $\boldsymbol{k}\cdot\boldsymbol{p}$ Kane model. The experimental Shubnikov–de Haas oscillations are also in good agreement with numerical simulations based on this model.

DOI: 10.1103/PhysRevB.70.115328 PACS number(s): 71.70.Ej, 73.21.−b, 72.20.My

I. INTRODUCTION

In general, level splitting due to structure inversion asymmetry (SIA), known as Rashba S−O splitting,[1,2] is inversely proportional to the energy gap. S−O coupling is relatively weak for *s*-like conduction bands and strong in *p*-like hole states. However, mixing of the conduction subbands with the valence subbands increases with decreasing energy gap. It has been shown that electrons in narrow-gap heterostructures, based on HgTe,[3] exhibit strong Rashba S−O coupling. In addition to the small energy gap in HgTe quantum wells (QW's), another important factor contributing to the large magnitude of the Rashba S−O coupling is the inverted band structure of HgTe QW's with well widths greater than 6 nm, in which the first conduction band has heavy-hole character.[3,4]

For possible applications in spintronics,[5,6] the Rashba effect has recently been investigated in a number of narrow-gap III-V systems[7–10] in which typical values of the Rashba S−O splitting energy, Δ_R, are 3–5 meV. Δ_R is appreciably larger in II-VI HgTe QW's, and values of 10–17 meV have been determined.[3,11,12] Zhang *et al.*[3] demonstrated that the Rashba S−O interaction is the dominant mechanism in such structures; they studied the strong dependence of S−O splitting on gate voltage and its subsequent disappearance when the QW was symmetric as expected for the Rashba effect. Recently strong Rashba S−O splitting has been reported for the surface state bands on low-index surfaces of Bi.[13]

Compared to the observation of a series of nodes in Shubnikov–de Haas (SdH) oscillations for an $In_{1-x}Ga_xAs$ heterostructure[14] at $B<1$ T, similar beating patterns are observable at higher magnetic fields in HgTe heterostructures[3] due to its larger Rashba effect.

In this article, we report on an investigation of beating patterns in the SdH oscillations in high-quality *n*-type $HgTe/Hg_{0.3}Cd_{0.7}Te$ QW's. Up to 12 nodes have been observed in the beating pattern within a magnetic field range of 0.9 T$<B<$6 T. A S−O splitting of ~30 meV due to the Rashba effect has been directly deduced from the node positions. This value is in good agreement with self-consistent Hartree calculations. The observed SdH oscillations and beating patterns are also in good agreement with the density of states, DOS, obtained from self-consistent $\boldsymbol{k}\cdot\boldsymbol{p}$ calculations.

II. EXPERIMENTAL DETAILS

Fully strained *n*-type $HgTe/Hg_{0.3}Cd_{0.7}Te(001)$ QW's were grown by molecular beam epitaxy (MBE) on $Cd_{0.96}Zn_{0.04}Te(001)$ substrates in a Riber 2300 MBE system. Details of the growth have been reported elsewhere.[3,15] Samples A and B are from the same chip, Q1772, which was modulation doped asymmetrically in the top barrier of the HgTe QW structure using CdI_2 as a doping material. The HgTe well width is 12.5 nm and the $Hg_{0.3}Cd_{0.7}Te$ barriers consist of a 5.5-nm-thick spacer and a 9-nm-thick doped layer. With a well width of 12.5 nm, the first conduction band in the QW has heavy-hole character—i.e., is a pure heavy-hole state at $\boldsymbol{k}=0$—and following standard nomenclature is labeled *H*1.

Standard Hall bars were fabricated by wet chemical etching. A 200-nm-thick Al_2O_3 film was deposited on top of the structure, which serves as an insulating layer. Finally Al was evaporated to form a metallic gate electrode on sample B. A metallic gate was not fabricated on sample A, which accounts for the different two-dimensional electron gas (2DEG) concentrations in these two samples. Ohmic indium contacts to the Hall bars were formed by thermal bonding.

Magnetotransport measurements were carried out in several different cryostats using dc techniques with currents of 1–5 μA in magnetic fields ranging up to 15 T and temperature from 1.4 to 35 K. During the measurement, the applied electric field was kept low enough to avoid excessive electron heating.[16]

III. THEORETICAL DETAILS

The band structure, Landau levels (LL's), and Rashba S−O splitting energy Δ_R were obtained from self-consistent

TABLE I. Band structure parameters employed in the calculations for HgTe and CdTe at $T=0$ K in the 8×8 $\boldsymbol{k}\cdot\boldsymbol{p}$ Kane model.

	E_g (eV)	Δ (eV)	E_p (eV)	F	γ_1	γ_2	γ_3	κ	ϵ
HgTe	−0.303	1.08	18.8	0	4.1	0.5	1.3	−0.4	21
CdTe	1.606	0.91	18.8	−0.09	1.47	−0.28	0.03	−1.31	10.4

Hartree calculations based on an 8×8 $\boldsymbol{k}\cdot\boldsymbol{p}$ band structure model including all second-order terms in the conduction- and valence-band blocks of the 8×8 Hamiltonian. In the calculations the inherent inversion asymmetry of HgTe and $Hg_{1-x}Cd_xTe$ has been neglected, because this effect has been shown to be very small in narrow-gap systems.[17,18] The envelope function approximation was used to calculate the subbands of the QW's and the influence of the induced free carriers has been included in a self-consistent Hartree calculation. The valence-band offset between HgTe and CdTe was taken to be 570 meV (Ref. 15) and to vary linearly with barrier composition.[19] The band structure parameters of HgTe and CdTe at 0 K employed in this investigation are listed in Table I and the model is described in detail elsewhere.[3,4]

IV. RESULTS AND DISCUSSION

Typical SdH oscillations are shown in Fig. 1 for sample A with a Hall concentration of 2.0×10^{12} cm^{-2} and a mobility of 9.5×10^4 cm^2/(V s) at 1.4 K. Oscillations can be resolved down to 0.8 T, indicating the excellent quality of the sample. Fast Fourier transformation (FFT) spectra of SdH oscillations are shown in Fig. 2(a) at various temperatures for sample A. The 2DEG concentrations of the S−O split $H1-$ and $H1+$ subbands are 0.80 and 1.06×10^{12} cm^{-2}, respectively, which are constant, within experimental uncertainties, for temperatures up to at least 35 K. The amplitudes of the two peaks have similar temperature behavior which can be described by[20]

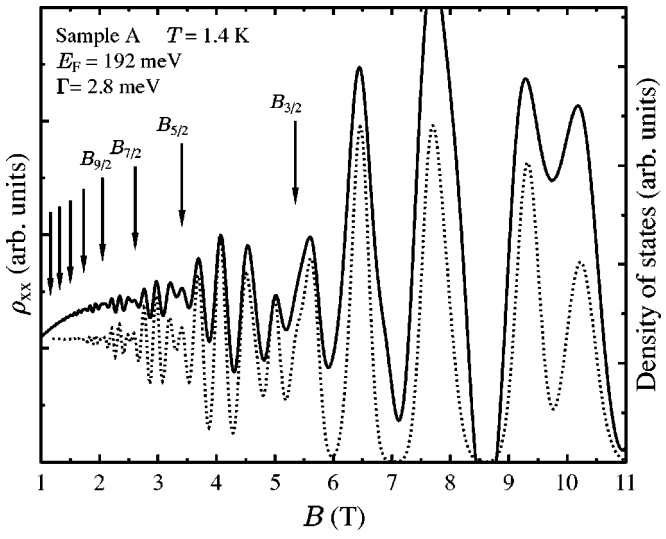

FIG. 1. SdH oscillations (solid curve) and calculated density of states (dotted curve) for sample A. A linear background has been subtracted from the experimental SdH results. Node positions in the beating patterns are indicated with arrows.

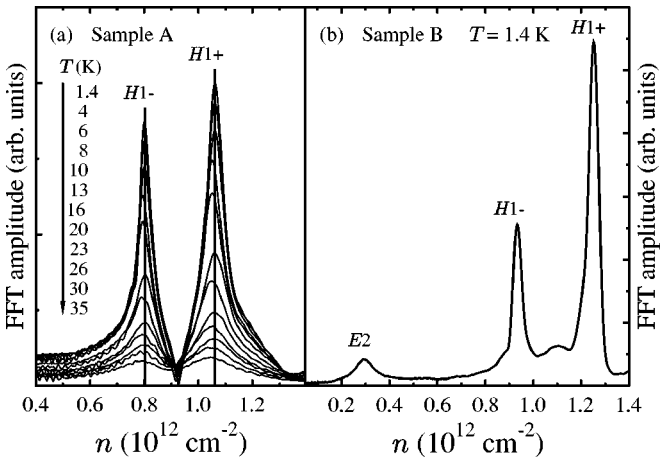

FIG. 2. (a) FFT of SdH oscillations of sample A for temperatures between 1.4 and 35 K. The vertical lines are merely guides to the eye indicating the electron concentrations for the $H1-$ and $H1+$ subbands. (b) FFT of SdH oscillations of sample B at 1.4 K.

$$A(T)=\frac{X}{\sinh(X)}, \tag{1}$$

where

$$X=2\pi^2\frac{k_BT}{\hbar\omega_c}. \tag{2}$$

From the temperature dependence of the SdH oscillation amplitudes, the effective electron mass at the Fermi level, m_F, was deduced to be $(0.044\pm0.005)m_e$ and $(0.050\pm0.005)m_e$ for samples A and B, respectively, where m_e is the free electron mass. These values are in good agreement with calculated effective electron masses of $0.049m_e$ and $0.053m_e$, respectively.

Beating patterns in the SdH oscillations are observed when $B>0.9$ T. In the presence of significant broadening of the LL's, the amplitude of the beat frequency will have a maximum in the vicinity of the intersection of two LL's. A node between two maxima will appear where only one LL is present—i.e., $\delta/\hbar\omega_c=(N+1/2)$, with $N=0,1,2\ldots$,—where δ is the total spin splitting and $\hbar\omega_c$ is the Landau level splitting.[21] The three observable quantum Hall plateaus directly below the node at 5.35 T correspond to even filling factors, whereas the three above correspond to odd filling factors. This node is due to the crossing point at $\delta=3/2\hbar\omega_c$.

Sample B has a higher electron concentration due to deposition of an insulating layer and metallic gate electrode which results in a different work function between the semiconductor and surface. In Fig. 3 the vertical arrows indicate the node positions of the SdH oscillations. Total electron concentration from the FFT of 2.76×10^{12} cm^{-2} ($n_{H1+}+n_{H1-}+2n_{E2}$), shown in Fig. 2(b), agrees well with the value

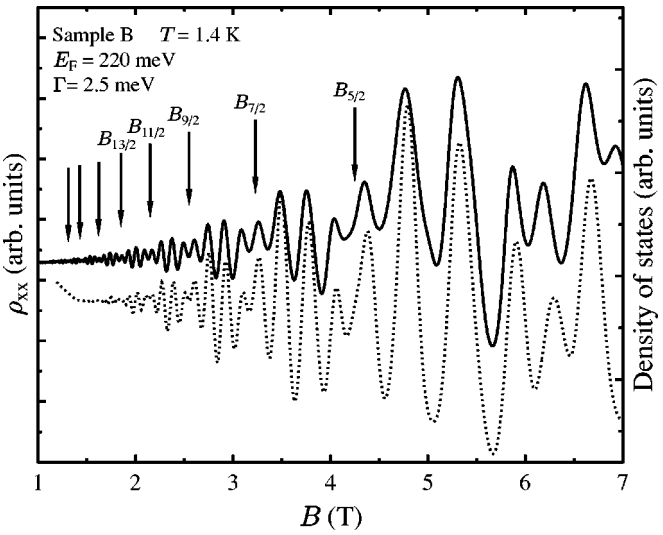

FIG. 3. SdH oscillations (solid curve) and calculated density of states (dotted curve) for sample B. A linear background has been subtracted from the experimental SdH results. Node positions in the beating patterns are indicated with arrows.

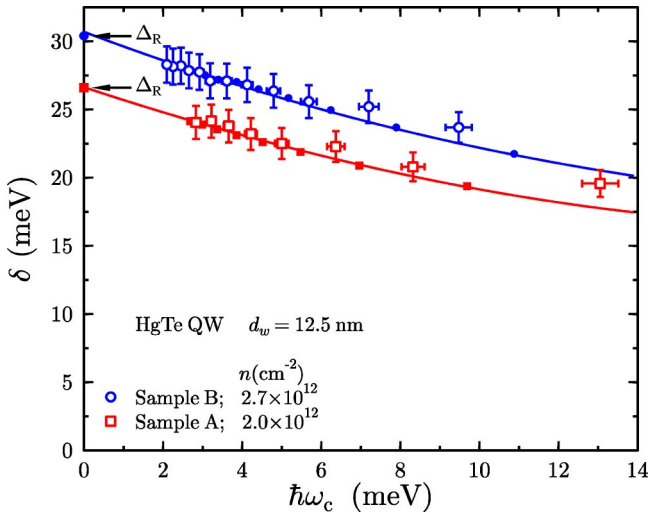

FIG. 4. Total experimental (open symbols) spin splitting energies and values calculated from the intersection of LL's (solid symbols) for samples A and B as a function of $\hbar\omega_c$. The numerically calculated Rashba S−O splitting energies at $B=0$ (solid symbols), Δ_R, are indicated by horizontal arrows. The lines are least-squares fits of the analysis of the self-consistently calculated LL's described in the text.

of 2.7×10^{12} cm^{-2} deduced from the low-magnetic-field Hall coefficient. From the ratio of the magnetic field strengths of all observed nodes, it has been determined that the node at 4.25 T for sample B corresponds to $\delta=5/2\hbar\omega_c$. Up to 12 beating nodes were observed for magnetic fields between 0.9 T and the highest field of 7.0 T. The second conduction subband $E2$ is also occupied; however, the expected weak splitting of this primarily s-like state of $\leqslant$0.2 meV was less than the experimental resolution.

The total spin splitting energy δ deduced from the node position in the beating patterns of the SdH oscillations is shown in Fig. 4 as a function of Landau splitting energy, $\hbar\omega_c$. When the LL's from the $H1$ subband intersect at or near the chemical potential as shown for sample A in Fig. 5, a maximum in the amplitude of the beat frequency occurs. δ can be determined from the intersection according to

$$E_{n_i}^{-} = E_{n_f}^{+}, \tag{3}$$

$$(n_i + 1/2)\hbar\omega_c + \delta = (n_f + 1/2)\hbar\omega_c, \tag{4}$$

$$\delta = \Delta n\hbar\omega_c. \tag{5}$$

The two crossing points in Fig. 5 correspond to a Δn of 2 and 3. The change in Landau quantum number for all pairs of LL's which intersect at or near the chemical potential is given by 1, 2, 3, 4, 5. … Even though the LL's with $\Delta n=1$ do intersect, they do so further removed from the chemical potential than the subsequent series of LL pairs. In order to increase the number of theoretical data points, the energy difference between appropriate LL's was employed when one LL was below the chemical potential and the other above. These values are in excellent agreement with those obtained from the intersection of LL's. A similar series of LL's crossing points exist for sample B, and the analysis of the LL's in the vicinity of the chemical potential described above also resulted in a consistent set of data.

Values of δ obtained from the intersection of LL's and a least squares fit of all theoretical data for both samples are plotted as a function of $\hbar\omega_c$ in Fig. 4 together with the experimental results. Obviously theory and experiment are in very good agreement with the exception of the $B_{3/2}$ node in the amplitude of the beat frequency for sample A, which

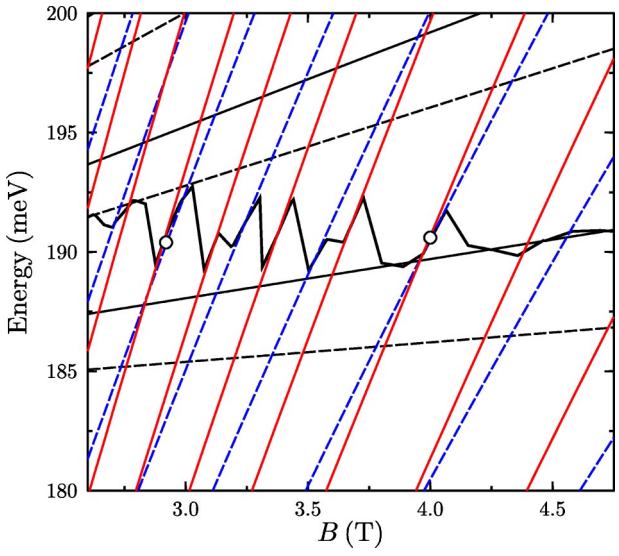

FIG. 5. Landau levels (LL's) for sample A between $B=2.6$ and 4.75 T near the chemical potential, which is reproduced as a thick line. The nearly vertical lines are LL's of the $H1$ conduction subband. The intersection of two LL's from the $H1$ conduction subband at the chemical potential are indicated with a circle. The nearly horizontal lines are LL's of the $E2$ conduction subband.

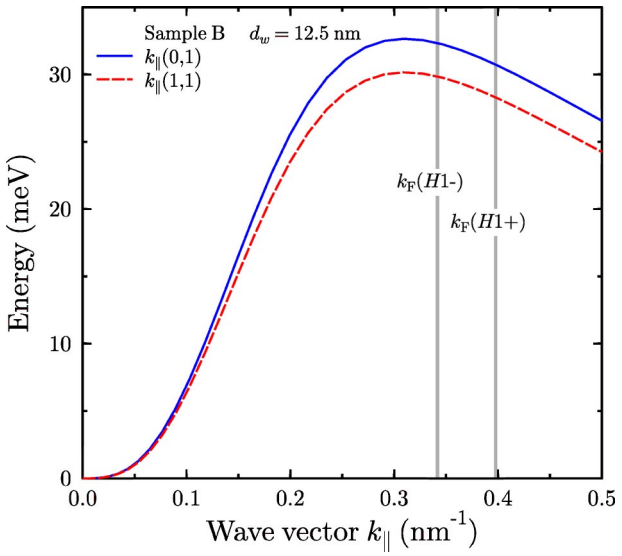

FIG. 6. Calculated spin splitting energy of the $H1$ subbands for sample B. The $\boldsymbol{k}$ vector for the $H1-$ and $H1+$ subbands at the Fermi surface are indicated by vertical lines.

corresponds to LL's with small filling factors.

The calculated Rashba S−O splitting energies Δ_R for sample B are 31.5 and 29.1 meV for the in-plane $k_\parallel(0,1)$ and $k_\parallel(1,1)$ vectors at the Fermi surface, respectively; see Fig. 6. Similarly the values for sample A are 27.5 and 25.4 meV, respectively. Δ_R values averaged over $\boldsymbol{k}_\parallel$ space of 26.5 and 30.4 meV for samples A and B are in good agreement with the experimentally determined total S−O splitting energies of 26 ± 1 and 30 ± 1 meV, respectively. The experimental splitting is due to the Rashba S−O effect, which results in the large population difference of 14.0% and 14.7% for samples A and B, respectively, shown in the FFT spectra in Fig. 2.

The Rashba S−O splitting energy of up to 30 meV in these HgTe QW's is almost one order of magnitude larger than the previously reported values in III-V compound semiconductors. This is due to the unique band structure of the HgTe system and in particular the inverted band structure. This value is also larger than previously reported values by Schultz *et al.*[11] and Zhang *et al.*[3] for HgTe-based QW's. This is mainly due to a larger 2DEG concentration in the $H1$ subband in the present QW's and the larger structure inversion asymmetry.

Experiments were also carried out in a tilted magnetic field for angles θ between 0° and 80°. The total spin splitting depends on the total magnetic field, whereas the SdH oscillations depend only on the perpendicular component of the magnetic field, $B_\perp$. Since S−O splitting is independent of the magnetic field and is much larger than Zeeman splitting at sufficiently low magnetic fields, $B_\perp$ values of the nodes are expected to be independent of θ at low magnetic fields. Experimentally the $B_\perp$ values required to produce a node are constant up to angles of $\theta\approx70°$ and then increase rapidly when the Zeeman splitting becomes comparable with the Rashba S−O splitting. This dependence on tilt angle demonstrates the 2D nature of the results in accordance with expectations for the Rashba effect and is similar to that reported in Ref. 14.

In order to compare the results of our self-consistent Hartree calculations with the measured longitudinal resistance, we have employed the following relationship to calculate the density of states (DOS) from the Landau level structure in the lowest-order cumulant approximation according to Gerhardts[22]:

$$D(\varepsilon_n^\pm) = \frac{1}{2\pi\lambda_c^2}\sum_{n\pm}\left[\frac{\pi}{2}\Gamma_n^2\right]^{-1/2}\exp\left[-2\frac{(E_F-\varepsilon_n^\pm)^2}{\Gamma_n^2}\right]. \quad (6)$$

Here $\varepsilon_n^\pm$ are the Landau level energies which are the result of our self-consistent Hartree calculations. $\lambda_c=\sqrt{\hbar/eB}$ is the usual magnetic length, and Γ_n is the Landau level broadening and is assumed to be a constant.

The experimental SdH oscillations and the numerical simulations of the DOS by means of Eq. (6) for samples A and B are reproduced in Figs. 1 and 3, respectively. The calculated Fermi energy was modified less than 1% in order to align the SdH oscillations. The best fit was obtained using $\Gamma=2.8$ meV for sample A and $\Gamma=2.5$ meV for sample B.

V. CONCLUSIONS

In conclusion, the beating patterns in the SdH oscillations of modulation-doped HgTe/$Hg_{0.3}Cd_{0.7}$Te QW's have been analyzed. The S−O splitting energy, which has been directly determined from the node positions to be as high as 30 meV, is almost one magnitude higher than that in InGaAs heterostructures with similar carrier densities. Self-consistent Hartree calculations based on an 8×8 $\boldsymbol{k}\cdot\boldsymbol{p}$ Hamiltonian have demonstrated that the experimental zero-field splitting energies are due to Rashba S−O splitting. Furthermore, good agreement between experimental SdH oscillations and calculated DOS is evidence that the Rashba term is the dominant mechanism of giant S−O splitting in HgTe QW's with an inverted band structure. This large Δ_R in HgTe QW's with an inverted band structure is caused by its narrow gap, the large spin-orbit gap between the bulk valence bands Γ_8^v and Γ_7^v, and the heavy-hole character of the first conduction subband. Furthermore, our calculations show that the method of directly deducing S−O splitting from node positions in SdH oscillations is applicable even for a system with a strongly nonparabolic band structure.

ACKNOWLEDGMENTS

The financial support of the major state basic research project No. G001CB3095 of China, National Natural Science Foundation of China (Grant No. 10374094), the Deutsche Forschungsgemeinschaft (Grant No. SFB410), BMBF, and the DARPA SpinS program is gratefully acknowledged.

*Electronic address: becker@physik.uni-wuerzburg.de

[1] E. I. Rashba, Fiz. Tverd. Tela (Leningrad) **2**, 1224 (1960) [Sov. Phys. Solid State **2**, 1109 (1960)]; Yu. A. Bychkov and E. I Rashba, Pis'ma Zh. Eksp. Teor. Fiz. **39**, 66 (1984) [JETP Lett. **39**, 78 (1984)].

[2] W. Zawadzki and P. Pfeffer, Semicond. Sci. Technol. **19**, R1-R17 (2004).

[3] X. C. Zhang, A. Pfeuffer-Jeschke, K. Ortner, V. Hock, H. Buhmann, C. R. Becker, and G. Landwehr, Phys. Rev. B **63**, 245305 (2001).

[4] A. Pfeuffer-Jeschke, Ph.D. thesis, Physikalisches Institut der Universität Würzburg, Germany, 2000.

[5] S. Datta and B. Das, Appl. Phys. Lett. **56**, 665 (1990).

[6] T. Koga, J. Nitta, H. Takayanagi, and S. Datta, Phys. Rev. Lett. **88**, 126601 (2002).

[7] J. Nitta, T. Akazaki, H. Takayanagi, and T. Enoki, Phys. Rev. Lett. **78**, 1335 (1997).

[8] G. Engels, J. Lange, Th. Schäpers, and H. Lüth, Phys. Rev. B **55**, R1958 (1997).

[9] C.-M. Hu, J. Nitta, T. Akazaki, H. Takayanagi, J. Osaka, P. Pfeffer, and W. Zawadzki, Phys. Rev. B **60**, 7736 (1999).

[10] D. Grundler, Phys. Rev. Lett. **84**, 6074 (2000).

[11] M. Schultz, F. Heinrichs, U. Merkt, T. Colin, T. Skauli, and S. Lóvold, Semicond. Sci. Technol. **11**, 1168 (1996).

[12] Y. S. Gui, C. R. Becker, J. Liu, V. Daumer, V. Hock, H. Buhmann, and L. W. Molenkamp, Europhys. Lett. **65**, 393 (2004).

[13] Yu. M. Koroteev, G. Bihlmayer, J. E. Gayone, E. V. Chulkov, S. Blügel, P. M. Echenique, and Ph. Hofmann, Phys. Rev. Lett. **93**, 046403 (2004).

[14] B. Das, D. C. Miller, S. Datta, R. Reifenberger, W. P. Hong, P. K. Bhattacharya, J. Singh, and M. Jaffe, Phys. Rev. B **39**, 1411 (1989).

[15] C. R. Becker, V. Latussek, A. Pfeuffer-Jeschke, G. Landwehr, and L. W. Molenkamp, Phys. Rev. B **62**, 10 353 (2000).

[16] Y. S. Gui, C. R. Becker, J. Liu, M. König, V. Daumer, M. N. Kiselev, H. Buhmann, and L. W. Molenkamp, cond-mat/0312424 (unpublished).

[17] M. H. Weiler, in *Semiconductors and Semimetals*, edited by R. Willardson and A. C. Beer (Academic Press, New York, 1981), Vol. 16, p. 119.

[18] U. Rössler, F. Malcher, and G. Lommer, *Spin-Splitting in Structured Semiconductors*, in Springer Series in Solid-State Sciences, Vol. 87, edited by G. Landwehr (Springer-Verlag, Berlin, 1989), p. 376.

[19] C. K. Shih and W. E. Spicer, Phys. Rev. Lett. **58**, 2594 (1987).

[20] P. T. Coleridge, Phys. Rev. B **44**, 3793 (1991).

[21] F. J. Teran, M. Potemski, D. K. Maude, T. Andrearczyk, J. Jaroszynski, and G. Karczewski, Phys. Rev. Lett. **88**, 186803 (2002).

[22] R. R. Gerhardts, Surf. Sci. **58**, 227 (1976).